BCSJ Award Article

Supramolecular Structures of Inclusion Complexes of C_{70} and Cyclic Porphyrin Dimers

Hirofumi Nobukuni,[1] Takuya Kamimura,[1] Hidemitsu Uno,[2] Yuichi Shimazaki,[3] Yoshinori Naruta,[1] and Fumito Tani*[1]

[1]Institute for Materials Chemistry and Engineering, Kyushu University, 6-10-1 Hakozaki, Higashi-ku, Fukuoka 812-8581

[2]Graduate School of Science and Engineering, Ehime University, Bunkyo-cho, Matsuyama, Ehime 790-8577

[3]College of Science, Ibaraki University, Bunkyo, Mito, Ibaraki 310-8512

Received August 17, 2011; E-mail: tanif@ms.ifoc.kyushu-u.ac.jp

Cyclic nickel and free-base porphyrin dimers (Ni_2-CPD_{Py} and H_4-CPD_{Py}) include fullerene C_{70} both in solution and in the crystals. Based on the ^{13}C NMR spectra in solution, the included C_{70} molecule inside the cavity of Ni_2-CPD_{Py} shows both end-on and side-on orientations, whereas the C_{70} molecule within H_4-CPD_{Py} has only a side-on orientation toward the porphyrin rings. X-ray crystallography revealed both "end-on" and "side-on" orientations of C_{70} in the crystal structure of the inclusion complex of Ni_2-CPD_{Py} and C_{70}. This is the first example of an X-ray crystallographic determination for an end-on orientation of C_{70} cocrystallized with porphyrins. On the other hand, only a side-on orientation of C_{70} was observed in the crystal structure of the complex of H_4-CPD_{Py} and C_{70}. Further, a zigzag array of C_{70} molecules through van der Waals contacts with each other is formed along the monoclinic *b* axis in the latter crystal.

Since the discovery and practical synthesis of C_{60} and C_{70},[1] much attention has been paid to the fullerene family in science and technology.[2] Next to C_{60}, C_{70} (Scheme 1) is the most stable and abundant fullerene. However, compared to C_{60}, the symmetry of C_{70} is lowered from I_h to D_h with an ellipsoidal shape of the longer (ca. 8.0 Å) and shorter (ca. 7.1 Å) axes. There has been a great interest in the relationship between the anisotropic structure and interactions of C_{70}, because electronic states of nano-carbon materials are generally dominated by forms and mutual interactions of their π planes.[3] For example, some reports suggest that carbon nanotubes including ellipsoidal C_{70} molecules inside their one-dimensional channels (so-called "peapod") have different electronic states depending upon the side-on and end-on orientations of encapsulated C_{70}.[4] However, it is still difficult to control the orientation of C_{70} in deliberate manner, because C_{70} is composed of only carbon atoms and has no functional groups.

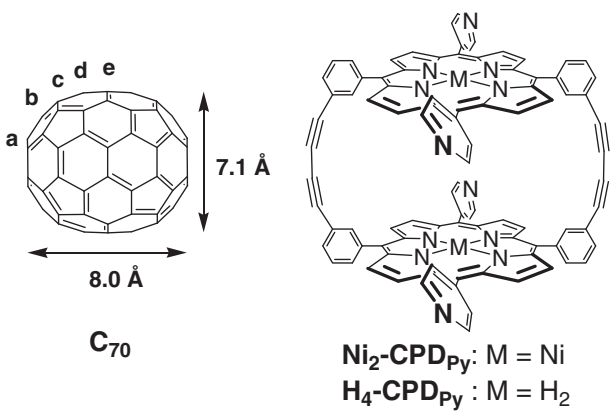

Scheme 1. Molecular structures of C_{70} and cyclic porphyrin dimers in this study.

One solution for this problem is to apply host–guest chemistry; that is, use of a suitable host fixing C_{70}. Porphyrin derivatives are particularly attractive components in the design of host molecules for fullerenes.[5] Many crystal structures of C_{70} cocrystallized with porphyrin monomers have been reported, and they all have shown side-on orientations of C_{70} toward porphyrin rings.[6] This tendency is originated from a result of maximizing the π–π interaction between the curved π planes of C_{70} and the flat π planes of porphyrins. On the other hand, there is no crystal structure for C_{70} included in porphyrin dimers except for the so-called jaws porphyrins,[7] although dimers generally have potentials to control the geometry of C_{70} due to their cavities of inherent shapes and sizes.[8] There has been only one report which demonstrated an end-on inclusion of C_{70} with an iridium porphyrin dimer in solution.[9]

Recently, we reported inclusion complexes composed of cyclic porphyrin dimers (CPD_{Py}, Scheme 1) and C_{60}.[10,11] The distance between the centers of the two porphyrin rings in the cyclic nickel porphyrin dimer (Ni_2-CPD_{Py}, 11.635 Å, Scheme 1) is comparable to the longer outer diameter of C_{70}

Published on the web November 29, 2011; doi:10.1246/bcsj.20110248

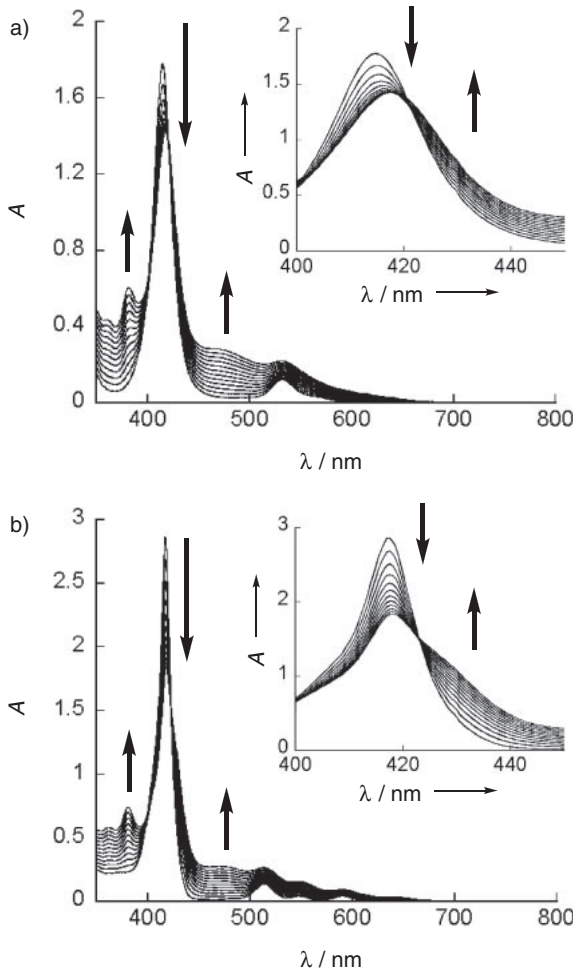

Figure 1. Absorption spectral changes of a) Ni_2-CPD_{Py} and b) H_4-CPD_{Py} upon titration with C_{70} in $CHCl_3$/toluene (1:1) at room temperature. The inset shows the Soret band region. $[CPD_{Py}] = 4.0 \times 10^{-6}$ M, $[C_{70}] = 1.1 \times 10^{-6}$–$1.2 \times 10^{-5}$ M.

(about 11.2 Å), and the corresponding distance in the cyclic free-base porphyrin dimer (H_4-CPD_{Py}, 10.785 Å, Scheme 1) is comparable to the shorter outer diameter of C_{70} (about 10.3 Å). Hence the inclusion of C_{70} inside the cavity of Ni_2-CPD_{Py} and H_4-CPD_{Py} is also expected. We herein report supramolecular structures of the inclusion complexes of Ni_2-CPD_{Py} and H_4-CPD_{Py} with C_{70}.

Results and Discussion

Inclusion of C_{70} by CPD_{Py} in Solution. Similarly to our previous study,[10a,11] we observed UV–vis absorption spectral changes during an addition of C_{70} to the solution of Ni_2-CPD_{Py} or H_4-CPD_{Py} in $CHCl_3$/toluene (1/1) at room temperature (Figure 1). The Soret absorption bands were red-shifted and decreased in intensity in both cases. The Job plot (415 nm) upon mixing of Ni_2-CPD_{Py} and C_{70} displayed a typical signature pattern for the formation of a 1:1 host–guest complex (C_{70}⊂Ni_2-CPD_{Py}).[12] The same plot of a mixture composed of H_4-CPD_{Py} and C_{70} also exhibited the formation of a 1:1 complex (C_{70}⊂H_4-CPD_{Py}).[12] On the basis of the titration of Ni_2-CPD_{Py} with C_{70}, the association constant (K_{assoc}) was

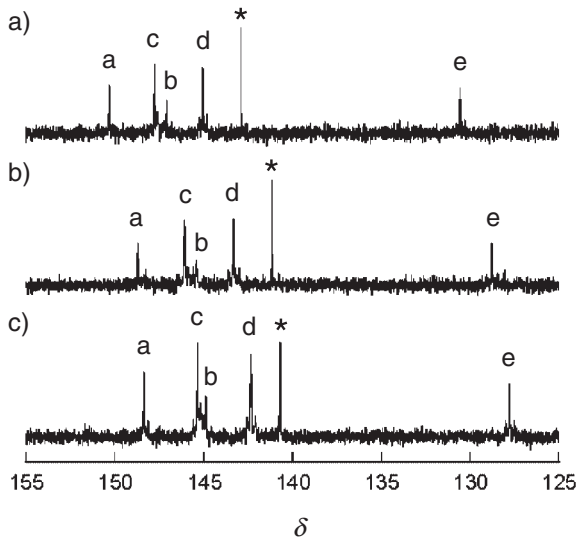

Figure 2. ^{13}C NMR spectra of a) ^{13}C-enriched C_{70} (2.0 mM), b) a mixture of Ni_2-CPD_{Py} (2.0 mM) and ^{13}C-enriched C_{70} (2.0 mM), and c) a mixture of H_4-CPD_{Py} (2.0 mM) and ^{13}C-enriched C_{70} (2.0 mM) in $CDCl_3/CS_2$ (1:1) at 20 °C. Asterisked signals originate from ^{13}C-enriched C_{60} as a contamination.

evaluated to be 1.2×10^6 M^{-1}.[12] This value is very close to that (1.2×10^6 M^{-1}) of the cyclic nickel porphyrin dimer linked by –$O(CH_2)_6O$– spacers rather than by butadiynyl groups,[8a] and almost one order of magnitude larger than that (2.0×10^5 M^{-1}) for C_{60} in Ni_2-CPD_{Py}.[10a] The K_{assoc} of C_{70}⊂H_4-CPD_{Py} was determined to be 3.9×10^5 M^{-1} by the same method.[12] This value is almost one order of magnitude larger than that (9.6×10^4 M^{-1}) for C_{60} in H_4-CPD_{Py}.[11] These higher affinities of CPD_{Py} for C_{70} than for C_{60} is assigned to the larger π plane of C_{70}. However, the affinity of H_4-CPD_{Py} for C_{70} is much smaller than that (2.1×10^7 M^{-1}) of the cyclic free-base porphyrin dimer with –$O(CH_2)_6O$– spacers,[8a] probably due to the smaller cavity of H_4-CPD_{Py}. Electrospray ionization mass spectra (ESI-MS) of C_{70}⊂Ni_2-CPD_{Py} and C_{70}⊂H_4-CPD_{Py} in CH_2Cl_2/MeOH/CH_3COOH (50/50/0.2) revealed peak clusters at m/z 2281.0 ($[Ni_2\text{-}CPD_{Py} + C_{70}]^+$) and 1140.3 ($[Ni_2\text{-}CPD_{Py} + C_{70}]^{2+}$), and at m/z 2165.8 ($[H_4\text{-}CPD_{Py} + C_{70}]^+$) and 1083.9 ($[H_4\text{-}CPD_{Py} + C_{70}]^{2+}$), respectively.[12] Additionally, both two spectra contained no peaks of free CPD_{Py} and C_{70}. All these spectroscopic data indicate the sufficient stability of the 1:1 complexation between CPD_{Py} and C_{70}.

Both C_{70}⊂Ni_2-CPD_{Py} and C_{70}⊂H_4-CPD_{Py} show highly symmetric ^{1}H NMR spectra in $CDCl_3$/benzene-d_6 (1/1) at room temperature (see Experimental section). It means that the included C_{70} molecule would oscillate in the cavity much faster than the NMR time scale and/or would be placed above the center of the porphyrin ring in solution. ^{13}C NMR spectroscopy is very informative of the C_{70} geometries with respect to porphyrin rings in C_{70}⊂Ni_2-CPD_{Py} and C_{70}⊂H_4-CPD_{Py} in solution. The pristine ^{13}C-enriched C_{70} in $CDCl_3/CS_2$ (1/1) at 20 °C (Figure 2a) shows five inequivalent ^{13}C NMR signals at $\delta_a = 150.27$, $\delta_b = 147.08$, $\delta_c = 147.75$, $\delta_d = 145.01$, $\delta_e = 130.55$ (alphabetical labelings are indicated in Scheme 1).

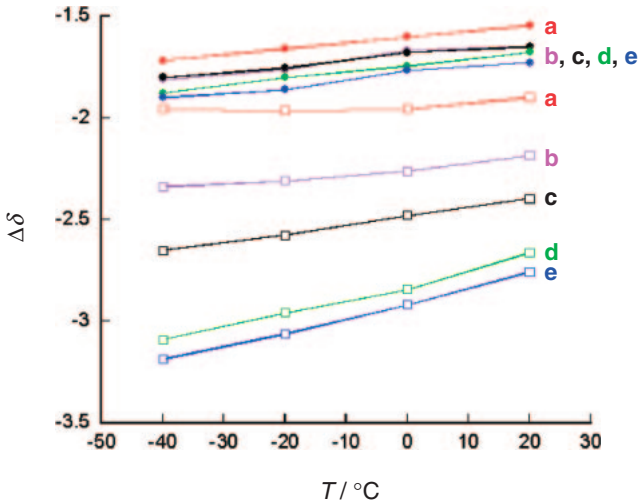

Figure 3. Chemical shift changes $\Delta\delta$ of signals a–e of C_{70} (2.0 mM) in ^{13}C NMR measurements after inclusion with Ni_2-CPD_{Py} (2.0 mM, circles) and H_4-CPD_{Py} (2.0 mM, squares) at −40 to 20 °C in $CDCl_3/CS_2$ (1:1).

When ^{13}C-enriched C_{70} was mixed with Ni_2-CPD_{Py} in $CDCl_3/CS_2$ (1/1) at 20 °C, all the C_{70} signals shifted up-field (Figures 2b and 3, $\Delta\delta_a = -1.54$, $\Delta\delta_b = -1.65$, $\Delta\delta_c = -1.65$, $\Delta\delta_d = -1.68$, $\Delta\delta_e = -1.73$), because of the ring current effect of the porphyrin rings. In the general cases of side-on C_{70} orientation with respect to porphyrin rings, the up-field shifts are more pronounced for the equatorial carbon atoms than for those at the poles, since the carbons at equatorial positions of C_{70} are nearer to the porphyrin rings than those at the pole positions.[7–9] The reverse phenomenon occurs, when C_{70} adopts an end-on orientation. However, in the case of $C_{70}\subset Ni_2$-CPD_{Py}, the up-field shifts for the five signals were almost equivalent. Therefore we concluded that the included C_{70} inside the cavity of Ni_2-CPD_{Py} has both side-on and end-on orientations in solution. On the other hand, for the mixture of ^{13}C-enriched C_{70} and H_4-CPD_{Py}, the differences of the up-field shifts of the C_{70} signals were much larger than those of $C_{70}\subset Ni_2$-CPD_{Py} (Figures 2c and 3, $\Delta\delta_a = -1.90$, $\Delta\delta_b = -2.18$, $\Delta\delta_c = -2.39$, $\Delta\delta_d = -2.66$, $\Delta\delta_e = -2.76$).[13] The more eminent up-field shifts for the equatorial carbons indicate that the carbons at the equatorial positions of the included C_{70} are closer to the porphyrin rings than those at the pole positions and that the main species of $C_{70}\subset H_4$-CPD_{Py} in solution has a side-on C_{70} orientation with respect to porphyrin rings.[7–9] Based on the ^{13}C NMR spectra and the crystal structures of these inclusion complexes (vide infra), it is thought that the behaviors of the included C_{70} molecules are mainly governed by the cavity sizes of the porphyrin dimers. The center-to-center distances of the porphyrin rings in the crystal structures are as follows: Ni_2-CPD_{Py} (11.635(1) Å),[10a] $C_{70}\subset Ni_2$-CPD_{Py} (11.960(1)–12.557(2) Å), H_4-CPD_{Py} (10.785 Å),[11] and $C_{70}\subset H_4$-CPD_{Py} (11.140 Å). In the larger cavity of Ni_2-CPD_{Py}, the included C_{70} molecule has a higher freedom of orientation. These trends of ^{13}C NMR spectra of $C_{70}\subset Ni_2$-CPD_{Py} and $C_{70}\subset H_4$-CPD_{Py} remain upon lowering temperature to −40 °C and all the signals are gradually more up-field shifted (Figure 3).

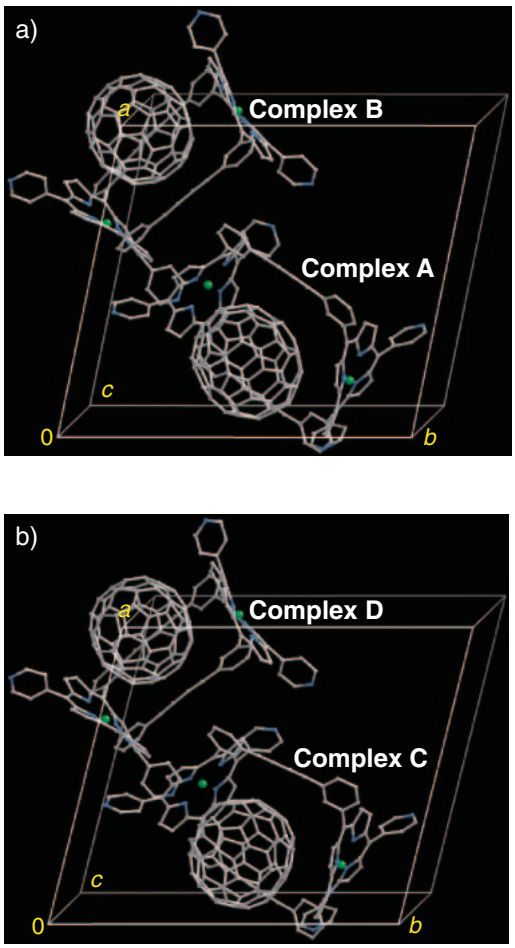

Figure 4. Wire frame depiction of the unit cell in the (a) crystal α and (b) crystal β of $C_{70}\subset Ni_2$-CPD_{Py}. Disordered minor structures, solvent molecules, and hydrogen atoms are omitted for clarity.

Crystal Structure of the Inclusion Complex of C_{70} and Ni_2-CPD_{Py}. We successfully revealed the supramolecular structures of $C_{70}\subset Ni_2$-CPD_{Py} by X-ray crystallography. Red single crystals of a 1:1 complex of C_{70} with Ni_2-CPD_{Py} were obtained by slow diffusion of hexane into a $CHCl_3$/toluene solution of a 1:1 mixture of C_{70} and Ni_2-CPD_{Py} at room temperature. Interestingly, $C_{70}\subset Ni_2$-CPD_{Py} shows crystal polymorphism, and there are two different crystals (crystal α and β, as shown in Figure 4). Furthermore, each crystal contains two crystallographically inequivalent inclusion complexes. Herein, the complexes in crystal α were named complex A and B (Figures 5a–5f), and the complexes in crystal β were named complex C and D (Figure S6 in the Suppporting Information).[12] It is remarkable that the C_{70} molecule in complex A shows an end-on orientation toward the porphyrin rings, while complexes B, C, and D have side-on C_{70} orientations. The crystal structure of complex A is the first example of an X-ray crystallographic determination for an end-on orientation of C_{70} cocrystallized with porphyrins. Although all the C_{70} molecules were treated as disordered structure, the orientations of the two disordered C_{70} molecules in each complex were almost the same. It means that the included C_{70} molecules can easily rotate around their longer axes inside the cavity of Ni_2-CPD_{Py}, and the

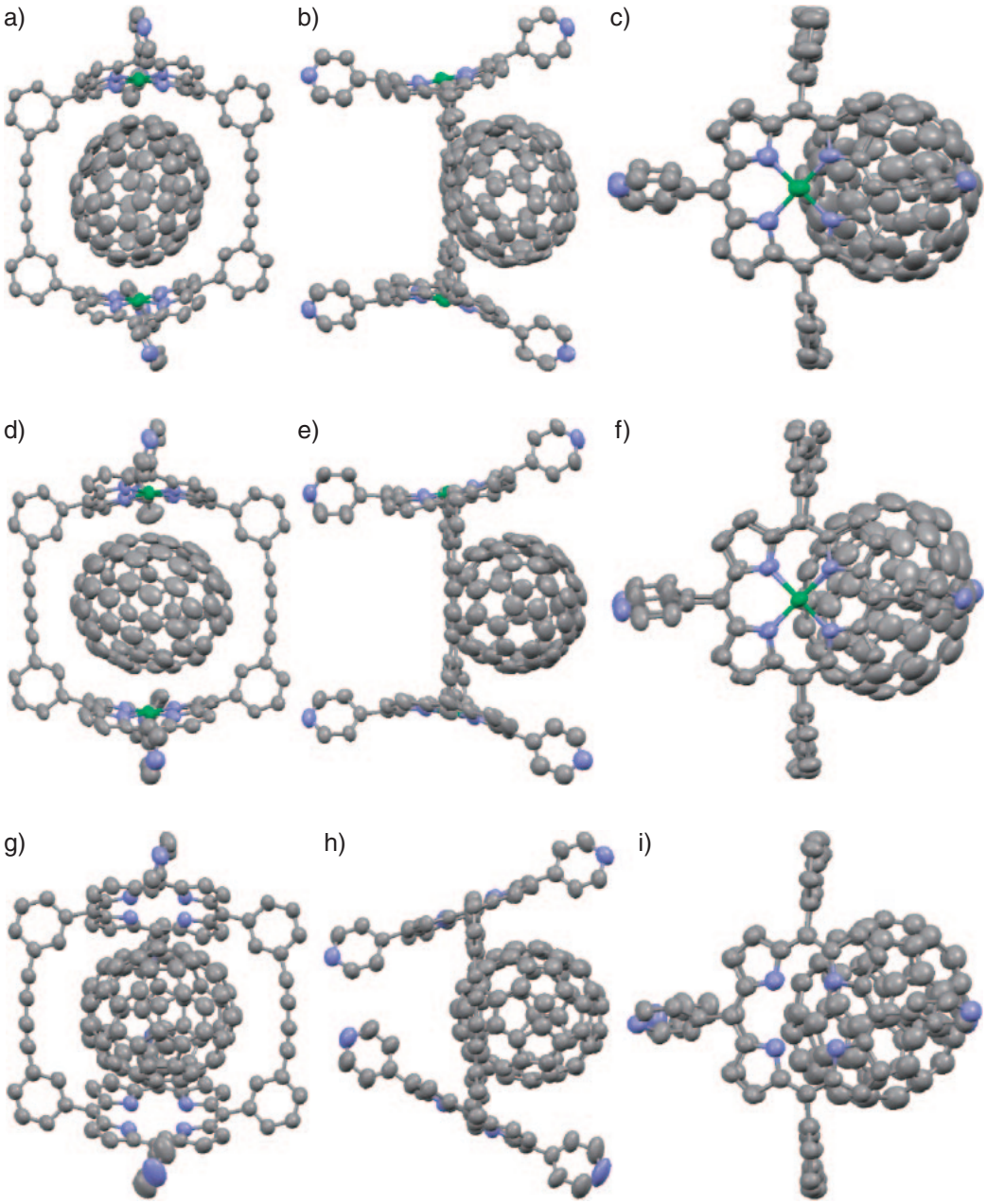

Figure 5. ORTEP of a–c) complex A (C_{70}⊂Ni_2-CPD_{Py}), d–f) complex B (C_{70}⊂Ni_2-CPD_{Py}), and g)–i) C_{70}⊂H_4-CPD_{Py} with 50% probability thermal ellipsoids. Disordered minor structures, solvent molecules, and hydrogen atoms are omitted for clarity. a), d), g) front view; b), e), h) side view; c), f), i) top view.

rotation around their shorter axes needs more activation energy. In comparison with the side-on orientation complexes B, C, and D, the Ni···Ni distance in complex A was slightly larger and the distance between the midpoints of butadiyne moieties in complex A was slightly smaller probably due to its end-on C_{70} orientation (Table 1). In the present all complexes, the C_{70} molecule is not located above the center of the porphyrin unit, because the size of the cavity is not large enough to accommodate C_{70} at the center. The similar off-center location of the fullerene molecule was observed in the crystal structure of the inclusion complex of C_{60} with Ni_2-CPD_{Py} (C_{60}⊂Ni_2-CPD_{Py}).[10a] The closest interactions in C_{70}⊂Ni_2-CPD_{Py} are π–π stacking between the C_{70} surface and the six-membered rings composed of a pyridyl-substituted meso carbon atom, two pyrrole α-carbon atoms, two pyrrole nitrogen atoms, and Ni ion. For example, in complex A, these π–π interactions have center-to-center distances of 4.225 and 3.614 Å, and dihedral angles of 29.67 and 13.34° (Figure 6). The similar interactions were also confirmed in the case of C_{60}⊂Ni_2-CPD_{Py}.[10a] In all the complexes, the dimers include C_{70} molecules with a clamshell-like conformation, in which the porphyrin rings are slightly tilted with respect to each other. A large number of low-spin four-coordinate Ni^{II} metalloporphyrins have been characterized by X-ray crystallography to show significantly ruffled conformations.[14] Similarly all the porphyrins in the crystal structures of C_{70}⊂Ni_2-CPD_{Py} are in ruffled conformations with

Table 1. Summary of the Crystal Structures of C_{70}⊂Ni_2-CPD_{Py}

	Complex A	Complex B	Complex C	Complex D
C_{70} orientation	End-on	Side-on	Side-on	Side-on
Ni···Ni/Å	12.557(2)	12.089(2)	11.960(1)	12.110(2)
Butadiyne···butadiyne[a]/Å	12.952	13.232	13.387	13.194
Ni···carbon of C_{70} (major)[b]/Å	3.57(1), 3.45(1)	3.60(1), 3.575(8)	3.35(1), 3.660(9)	3.58(1), 3.589(8)
Ni···carbon of C_{70} (minor)[b]/Å	3.66(2), 3.70(3)	3.56(3), 3.64(4)	3.31(2), 3.71(2)	3.55(2), 3.72(2)
π–π interaction distance (major)[c]/Å	4.225, 3.614	3.649, 3.597	3.648, 3.511	3.608, 3.674
π–π interaction distance (minor)[c]/Å	3.848, 3.565	3.648, 3.862	3.721, 3.960	3.920, 3.735
π–π interaction dihedral angle (major)[d]/°	29.67, 13.34	12.27, 11.32	8.36, 8.51	9.31, 11.77
π–π interaction dihedral angle (minor)[d]/°	18.60, 6.14	13.09, 11.28	10.69, 20.79	20.48, 13.16
Occupancy of major C_{70}	0.693(4)	0.777(5)	0.683(4)	0.758(4)

a) The distance between midpoints of butadiyne moieties. b) The shortest distances between Ni ions and carbon atoms of the C_{70} molecules. c) The shortest distances between the center of the six-membered ring in the C_{70} molecules and the center of the six-membered ring composed of a pyridyl-substituted meso carbon atom, two pyrrole α-carbon atoms, two pyrrole nitrogen atoms, and Ni ion in the porphyrin rings. d) The dihedral angles between the mean plane of the six-membered ring in the C_{70} molecules and the mean plane of the six-membered ring composed of a pyridyl-substituted meso carbon atom, two pyrrole α-carbon atoms, two pyrrole nitrogen atoms, and Ni ion in the porphyrin rings.

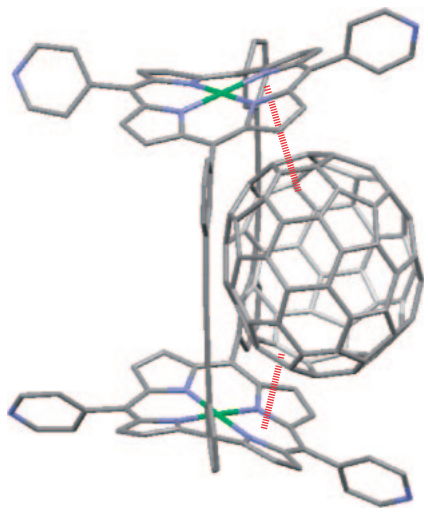

Figure 6. Details of the noncovalent interactions between Ni_2-CPD_{Py} and C_{70} in complex A. Disordered minor structures and hydrogen atoms are omitted for clarity. N: blue; Ni: green; C: gray.

alternating displacements of meso carbon atoms above and below the mean plane formed by the four nitrogen atoms,[15] which is the same feature as that of C_{60}⊂Ni_2-CPD_{Py}.[10a] The meso carbon atoms with the pyridyl substituents are displaced outward and the other meso carbon atoms are displaced inward. But there are some clear differences of the porphyrin conformation in the crystal structures between C_{70}⊂Ni_2-CPD_{Py} and C_{60}⊂Ni_2-CPD_{Py}. In all the crystal structures of C_{70}⊂Ni_2-CPD_{Py}, the two porphyrin rings are not rotated around the center-to-center axis (Figures 5c, 5f, S6c, and S6f),[12] and the butadiyne moieties are coplanar (Figures 5b, 5e, S6b, and S6e),[12] whereas the two porphyrin rings in C_{60}⊂Ni_2-CPD_{Py} are rotated around the center-to-center axis by 24.3° with respect to each other and the two butadiyne moieties are not coplanar.[10a]

Crystal Structure of the Inclusion Complex of C_{70} and H_4-CPD_{Py}. Black single crystals of C_{70}⊂H_4-CPD_{Py} were prepared by slow diffusion of hexane into a CH_2Cl_2/*o*-dichlorobenzene solution of a 1:1 mixture of C_{70} and H_4-CPD_{Py} at room temperature. X-ray crystallography revealed a 1:1 inclusion complex of C_{70} with H_4-CPD_{Py} (Figures 5g–5i). The included C_{70} molecule shows a side-on orientation toward the porphyrin rings as confirmed in solution. The features of this crystal structure are similar to those of the inclusion complex of C_{60} with H_4-CPD_{Py} (C_{60}⊂H_4-CPD_{Py}).[11] The porphyrin rings of C_{70}⊂H_4-CPD_{Py} show a higher planarity than C_{70}⊂Ni_2-CPD_{Py}; the displacements of the meso carbon atoms from the four-nitrogen mean plane are −0.228, 0.177, −0.305, −0.023, −0.294, −0.113, −0.193, and −0.014 Å (positive values meaning outward). The dimer bites the C_{70} molecule in a clamshell-like conformation, in which the flat porphyrin rings are tilted with respect to each other. The dihedral angle and the center-to-center distance of the two porphyrin planes are 51.57° and 11.140 Å, respectively. This large dihedral angle results in the close proximity of the two pyridyl groups in the opposite side of the C_{70} inclusion site (Figure S8).[12] The shortest carbon–carbon distance of the two pyridyl groups is 3.51(1) Å. Their steric hindrance would limit the dihedral angle and the center-to-center distance to hamper an end-on orientation of the included C_{70} molecule.[16] The distance between the midpoints of the butadiyne moieties, that is, the width of the cavity is 14.009 Å. These structural parameters are very close to those of C_{60}⊂H_4-CPD_{Py} (the dihedral angle: 52.38°, the center-to-center distance: 11.126 Å, the shortest C–C distance of Py: 3.778(7) Å, the cavity width 13.915 Å).[11] The shortest separations between the carbon atoms of C_{70} and the porphyrin centers are 2.990 and 2.851 Å (Figure 7). These values represent fairly strong π–π interactions between the porphyrins and C_{70}.

Moreover, the C_{70} molecules form a zigzag chain along the crystallographic *b* axis in the crystal packing (Figure 8). In this chain, the longer axes of C_{70} molecules are almost parallel to the axis of the zigzag array. The distance between the centers of the adjacent C_{70} molecules along the zigzag array (arrow A in Figure 8a) is 10.635 Å. This value is comparable to the shorter outer diameter of C_{70} (ca. 10.3 Å). In other words, the C_{70} molecules have van der Waals contacts with each other along

the zigzag arrangement. This zigzag array is derived from a partial covering of H_4-CPD_{Py}. The uncovered π plane of the three-dimensional and symmetric C_{70} molecule (rather than two-dimensional common aromatic compounds) enables these interesting interactions. The distances between the centers of the C_{70} molecules along the parallel direction to *b* axis (arrow B) and in the adjacent zigzag arrays (arrows C and D) are 14.887, 22.020, and 16.385 Å, respectively. The two porphyrin rings facing each other along the *c* axis show a strong π–π interaction with the shortest nitrogen–nitrogen distance of 3.446(5) Å (arrow E in Figure 8a).

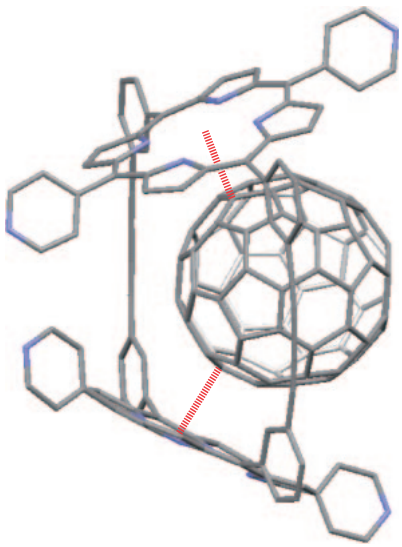

Figure 7. Details of the noncovalent interactions between H_4-CPD_{Py} and C_{70}. Disordered minor structures and hydrogen atoms are omitted for clarity. N: blue; C: gray.

Conclusion

The formation of 1:1 inclusion complexes of fullerene C_{70} with the cyclic nickel porphyrin dimer (Ni_2-CPD_{Py}) and the cyclic free-base porphyrin dimer (H_4-CPD_{Py}) was confirmed both in solution and in the crystals. The ^{13}C NMR spectra in the solution of $C_{70}\subset Ni_2$-CPD_{Py} revealed that the included C_{70} molecule takes both side-on and end-on orientations toward the porphyrin rings. On the contrary, the C_{70} molecule in H_4-CPD_{Py} has only a side-on orientation. $C_{70}\subset Ni_2$-CPD_{Py} shows crystal polymorphism and the two kinds of single crystal (crystal α and β) were obtained. Each crystal contains two crystallographically inequivalent inclusion complexes. On the whole, the four kinds of inclusion complex (complexes A, B, C, and D) were crystallographically analyzed. The C_{70} molecule in complex A shows an end-on C_{70} orientation, while complexes B, C, and D have side-on orientations. Especially, complex A is the first example of an X-ray crystallographic determination for an end-on orientation of C_{70} cocrystallized with porphyrins. On the other hand, $C_{70}\subset H_4$-CPD_{Py} does not show crystal polymorphism. Only a side-on orientation of the included C_{70} molecule is observed in the crystal structure of $C_{70}\subset H_4$-CPD_{Py}. Additionally, it is notable that in the crystal packing of $C_{70}\subset H_4$-CPD_{Py}, the zigzag array of the C_{70} molecules is formed with van der Waals contacts with each other inside the spaces surrounded by the porphyrin moieties. The orientation of the included C_{70} molecules is mainly dominated by the cavity sizes of the porphyrin dimers. The ruffled conformations of the porphyrins in $C_{70}\subset Ni_2$-CPD_{Py} lead to the outward displacements of the pyridyl groups and the expansion of the cavity. The C_{70} molecule in the larger cavity of Ni_2-CPD_{Py} has a higher freedom and takes both end-on and side-on orientations in solution and crystalline state, whereas the C_{70} molecule in the smaller cavity of H_4-CPD_{Py} is allowed to adopt only a

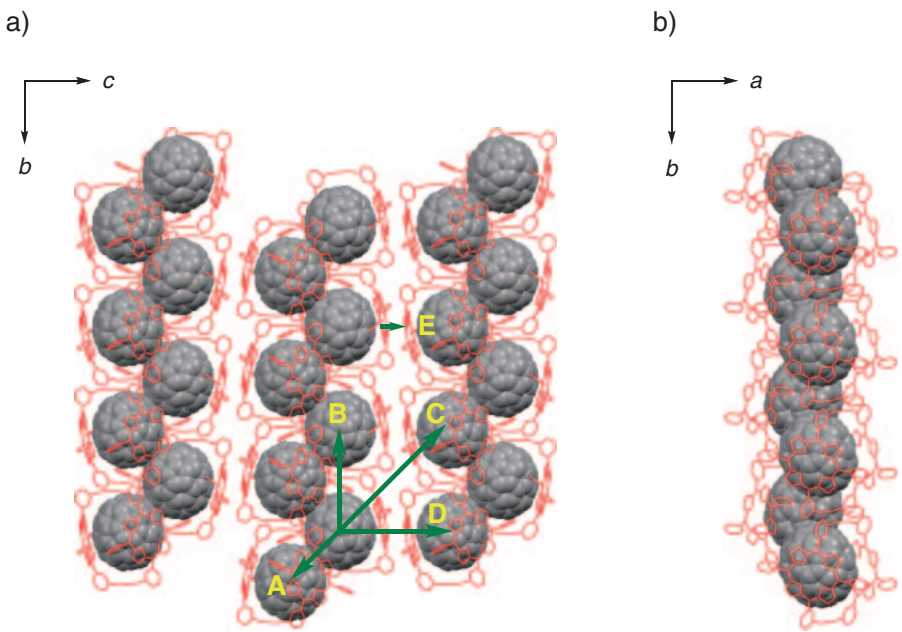

Figure 8. Zigzag arrays of $C_{70}\subset H_4$-CPD_{Py} in the crystal structures. The H_4-CPD_{Py} units and the C_{70} molecules are depicted by wire frames and space-filling models, respectively. Disordered minor structures, solvent molecules, and hydrogen atoms are omitted for clarity. a) Top view; b) side view.

side-on orientation. These results will contribute to the design of host molecules to control the anisotropic interactions of C_{70} in supramolecular structures.

Experimental

Materials. All reagents and solvents were purchased from commercial suppliers as the best grade available, and were used without further purification. The syntheses of Ni_2-CPD_{Py} and H_4-CPD_{Py} were performed in accordance with literature procedures.[10a,11]

Instruments. ^1H and ^{13}C NMR spectra were recorded on a JEOL ECS-400 (400 MHz) and JEOL ECA-500 (500 MHz) spectrometer. Chemical shifts were reported as δ values in ppm relative to tetramethylsilane. UV–vis absorption and IR spectra were recorded on Shimadzu UV-3100PC and BIO RAD FTS6000 spectrophotometers, respectively. ESI-MS was carried out on a Perkin-Elmer Sciex API 300 mass spectrometer.

C_{70}⊂Ni_2-CPD_{Py}. ^1H NMR ($CDCl_3$/benzene-d_6 (1:1), 500 MHz): δ 7.33 (s, 4H, Ar–H), 7.45 (t, $J = 7.7$ Hz, 4H, Ar–H), 7.54–7.55 (br-m, 4H + 8H, Ar–H + Ar–H), 8.35 (d, $J = 6.3$ Hz, 4H, Ar–H), 8.45 (d, $J = 5.2$ Hz, 8H, pyrrole β-H), 8.53 (d, $J = 3.4$ Hz, 8H, pyrrole β-H), 8.69 (d, $J = 4.0$ Hz, 8H, Ar–H); IR (KBr): $\nu = 1701$, 1593, 1464, 1430, 1404, 1354, 1283, 1134, 1076, 1007, 794, 711, 671, 642, 578, 566, 536, 459 cm^{-1}; elemental analysis calcd for $C_{92}H_{48}N_{12}Ni_2 \cdot C_{70} \cdot CHCl_3 \cdot H_2O$: C, 81.00; H, 2.13; N, 6.95%. Found: C, 80.94; H, 2.47; N, 6.79%.

C_{70}⊂H_4-CPD_{Py}. ^1H NMR ($CDCl_3$/benzene-d_6 (1:1), 400 MHz): δ −2.97 (br-s, 4H, –NH), 7.27 (s, 4H, Ar–H), 7.51 (t, $J = 7.7$ Hz, 4H, Ar–H), 7.56 (d, $J = 8.3$ Hz, 4H, Ar–H), 7.61 (br-s, 8H, Ar–H), 8.46 (d, $J = 7.3$ Hz, 4H, Ar–H), 8.54 (d, $J = 4.6$ Hz, 8H, pyrrole β-H), 8.65 (d, $J = 4.9$ Hz, 8H, pyrrole β-H), 8.85 (br-s, 8H, Ar–H); IR (KBr): $\nu = 1591$, 1474, 1429, 1400, 1136, 974, 881, 797, 725, 675, 660, 642, 579, 565, 536, 459 cm^{-1}; elemental analysis calcd for $C_{92}H_{52}N_{12} \cdot C_{70} \cdot (C_6H_4Cl_2)_3$: C, 82.92; H, 2.47; N, 6.45%. Found: C, 82.98; H, 2.60; N, 6.52%.

X-ray Structure Determination. X-ray crystallography was carried out on single crystals of C_{70}⊂Ni_2-CPD_{Py} (crystal α and β) and C_{70}⊂H_4-CPD_{Py} by using a Rigaku RAXIS imaging plate area detector with graphite monochromated Mo Kα radiation ($\lambda = 0.71075$ Å) and Cu Kα radiation ($\lambda = 1.54187$ Å), respectively. The crystals were mounted on a glass fiber. To determine the cell constants and orientation matrix, three oscillation photographs were taken for each frame, with an oscillation angle of 3° and an exposure time of 3 min. Reflection data were corrected for both Lorentz and polarization effects. The structures were solved by direct methods (SIR-2004)[17] with the Crystal Structure[18] crystallographic software package, and refined by full-matrix least-squares procedures on F^2 for all reflections (SHELXL-97).[19] Non-hydrogen atoms were refined anisotropically. Hydrogen atoms were refined by using the rigid model. In all the crystals, some solvent molecules, such as chloroform, dichloromethane, toluene, hexane, and *o*-dichlorobenzene were not properly modeled. Therefore, the structures were refined without these solvents by PLATON Squeeze technique.[20] The final structures were validated by using PLATON cif check. X-ray crystal structure data for crystal α (C_{70}⊂Ni_2-CPD_{Py}): $C_{92}H_{48}N_{12}Ni_2 \cdot C_{70}$; red crystal; dimensions $0.65 \times 0.26 \times 0.10$ mm^3; triclinic; space group $P\bar{1}$; $a = 22.942(4)$, $b = 24.631(3)$, $c = 25.570(4)$ Å; $\alpha = 82.337(5)$, $\beta = 68.546(6)$, $\gamma = 78.175(5)°$; $V = 13136(3)$ $Å^3$; $Z = 4$; $\rho_{calcd} = 1.153$ g cm^{-3}; $2\theta_{max} = 54.98°$; $T = 133$ K; 214217 reflections collected; 59238 reflections used and 3781 parameters. $R_1 = 0.0987$ ($I > 2.0\sigma(I)$), $R_w = 0.2141$ (all data). Crystal β (C_{70}⊂Ni_2-CPD_{Py}): $C_{92}H_{48}N_{12}Ni_2 \cdot C_{70}$; red crystal; dimensions $0.68 \times 0.18 \times 0.06$ mm^3; triclinic; space group $P\bar{1}$; $a = 22.461(4)$, $b = 24.819(3)$, $c = 25.924(4)$ Å; $\alpha = 81.635(4)$, $\beta = 69.615(6)$, $\gamma = 75.641(6)°$; $V = 13095(4)$ $Å^3$; $Z = 4$; $\rho_{calcd} = 1.156$ g cm^{-3}; $2\theta_{max} = 54.98°$; $T = 133$ K; 211569 reflections collected; 59317 reflections used and 3805 parameters. $R_1 = 0.0872$ ($I > 2.0\sigma(I)$), $R_w = 0.1820$ (all data). C_{70}⊂H_4-CPD_{Py}: $C_{92}H_{52}N_{12} \cdot C_{70}$; black crystal; dimensions $0.20 \times 0.20 \times 0.07$ mm^3; monoclinic; space group $P2_1/c$; $a = 17.1837(3)$, $b = 14.8868(3)$, $c = 47.1613(9)$ Å; $\beta = 91.6385(8)°$; $V = 12059.3(4)$ $Å^3$; $Z = 4$; $\rho_{calcd} = 1.193$ g cm^{-3}; $2\theta_{max} = 136.50°$; $T = 100$ K; 218443 reflections collected; 22077 reflections used and 2010 parameters. $R_1 = 0.0911$ ($I > 2.0\sigma(I)$), $R_w = 0.1823$ (all data). Crystallographic data have been deposited with Cambridge Crystallographic Data Centre: Deposition number CCDC-810786, 810787 for C_{70}⊂Ni_2-CPD_{Py}, and 837455 for C_{70}⊂H_4-CPD_{Py}. Copies of the data can be obtained free of charge via http://www.ccdc.cam.ac.uk/conts/retrieving.html (or from the Cambridge Crystallographic Data Centre, 12, Union Road, Cambridge, CB2 1EZ, U.K.; Fax: +44 1223 336033; e-mail: deposit@ccdc.cam.ac.uk).

This work was supported by Grants-in-Aid (Scientific Research on Innovative Areas No. 20108009 to F.T., "pi-Space," and the Global COE Program "Science for Future Molecular Systems") from the Ministry of Education, Culture, Sports, Science and Technology of Japan, by the Cooperative Research Program of "Network Joint Research Center for Materials and Devices (Institute for Materials Chemistry and Engineering, Kyushu University)," and by a Research Grant to F.T. from Tokuyama Science Foundation. H. N. acknowledges the Japan Society for the Promotion of Science (JSPS) for a Research Fellowship for Young Scientists.

Supporting Information

Additional spectroscopic and crystallographic data. This material is available free of charge on the Web at http://www.csj.jp/journals/bcsj/.

References

1 a) H. W. Kroto, J. R. Heath, S. C. O'Brien, R. F. Curl, R. E. Smalley, *Nature* **1985**, *318*, 162. b) W. Krätschmer, L. D. Lamb, K. Fostiropoulos, D. R. Huffman, *Nature* **1990**, *347*, 354.

2 *Fullerenes: Chemistry, Physics, and Technology*, ed. by K. M. Kadish, R. S. Ruoff, Wiley, New York, **2000**.

3 a) Y.-B. Wang, Z. Lin, *J. Am. Chem. Soc.* **2003**, *125*, 6072. b) A. Goldoni, C. Cepek, R. Larciprete, L. Sangaletti, S. Pagliara, L. Floreano, R. Gotter, A. Verdini, A. Morgante, Y. Luo, M. Nyberg, *J. Chem. Phys.* **2002**, *116*, 7685. c) R. C. Haddon, *Acc. Chem. Res.* **1992**, *25*, 127.

4 a) S. Okubo, T. Okazaki, K. Hirose-Takai, K. Suenaga, S. Okada, S. Bandow, S. Iijima, *J. Am. Chem. Soc.* **2010**, *132*, 15252.

b) K. Hirahara, S. Bandow, K. Suenaga, H. Kato, T. Okazaki, H. Shinohara, S. Iijima, *Phys. Rev. B* **2001**, *64*, 115420. c) M. Otani, S. Okada, A. Oshiyama, *Phys. Rev. B* **2003**, *68*, 125424.

5 a) K. Tashiro, T. Aida, *Chem. Soc. Rev.* **2007**, *36*, 189. b) P. D. W. Boyd, C. A. Reed, *Acc. Chem. Res.* **2005**, *38*, 235.

6 a) T. Ishii, N. Aizawa, R. Kanehama, M. Yamashita, K.-i. Sugiura, H. Miyasaka, *Coord. Chem. Rev.* **2002**, *226*, 113. b) D. V. Konarev, I. S. Neretin, Y. L. Slovokhotov, E. I. Yudanova, N. V. Drichko, Y. M. Shul'ga, B. P. Tarasov, L. L. Gumanov, A. S. Batsanov, J. A. K. Howard, R. N. Lyubovskaya, *Chem.—Eur. J.* **2001**, *7*, 2605. c) P. D. W. Boyd, M. C. Hodgson, C. E. F. Rickard, A. G. Oliver, L. Chaker, P. J. Brothers, R. D. Bolskar, F. S. Tham, C. A. Reed, *J. Am. Chem. Soc.* **1999**, *121*, 10487. d) M. M. Olmstead, D. A. Costa, K. Maitra, B. C. Noll, S. L. Phillips, P. M. Van Calcar, A. L. Balch, *J. Am. Chem. Soc.* **1999**, *121*, 7090.

7 a) D. Sun, F. S. Tham, C. A. Reed, L. Chaker, M. Burgess, P. D. W. Boyd, *J. Am. Chem. Soc.* **2000**, *122*, 10704. b) D. Sun, F. S. Tham, C. A. Reed, L. Chaker, P. D. W. Boyd, *J. Am. Chem. Soc.* **2002**, *124*, 6604.

8 a) J.-Y. Zheng, K. Tashiro, Y. Hirabayashi, K. Kinbara, K. Saigo, T. Aida, S. Sakamoto, K. Yamaguchi, *Angew. Chem., Int. Ed.* **2001**, *40*, 1857. b) A. Ouchi, K. Tashiro, K. Yamaguchi, T. Tsuchiya, T. Akasaka, T. Aida, *Angew. Chem., Int. Ed.* **2006**, *45*, 3542.

9 M. Yanagisawa, K. Tashiro, M. Yamasaki, T. Aida, *J. Am. Chem. Soc.* **2007**, *129*, 11912.

10 a) H. Nobukuni, Y. Shimazaki, F. Tani, Y. Naruta, *Angew. Chem., Int. Ed.* **2007**, *46*, 8975. b) H. Nobukuni, F. Tani, Y. Shimazaki, Y. Naruta, K. Ohkubo, T. Nakanishi, T. Kojima, S. Fukuzumi, S. Seki, *J. Phys. Chem. C* **2009**, *113*, 19694.

11 H. Nobukuni, Y. Shimazaki, H. Uno, Y. Naruta, K. Ohkubo, T. Kojima, S. Fukuzumi, S. Seki, H. Sakai, T. Hasobe, F. Tani, *Chem.—Eur. J.* **2010**, *16*, 11611.

12 See the Supporting Information.

13 Every up-field shift of $C_{70}\subset H_4$-CPD_{Py} was larger than the corresponding resonance of $C_{70}\subset Ni_2$-CPD_{Py}. The same tendency was also observed for the ^{13}C NMR spectra of $C_{60}\subset Ni_2$-CPD_{Py} ($\Delta\delta = -1.69$)[10a] and $C_{60}\subset H_4$-CPD_{Py} ($\Delta\delta = -2.35$).[11] It is rather difficult to assign the exact reasons of this tendency because the detailed solution structures of these inclusion complexes have not been clarified. One of the possible reasons is that the higher planarity of the porphyrin rings of H_4-CPD_{Py} than that of Ni_2-CPD_{Py} (vide infra) would induce more obvious ring-current effect in the NMR spectra.

14 W. R. Sheidt, in *The Porphyrin Handbook*, ed. by K. M. Kadish, K. M. Smith, R. Guilard, Academic Press, San Diego, **2000**, Vol. 3, pp. 49–112.

15 In the crystal structures of complexes A, B, C, and D, the displacements of the meso carbon atoms from the four-nitrogen mean plane are as follows: complex A (−0.632, 0.622, −0.636, 0.503, −0.628, 0.656, −0.600, and 0.511 Å), complex B (−0.553, 0.452, −0.469, 0.451, −0.394, 0.529, −0.586, and 0.436 Å), complex C (−0.495, 0.537, −0.547, 0.407, −0.535, 0.597, −0.493, and 0.473 Å), complex D (−0.532, 0.457, −0.434, 0.448, −0.473, 0.538, −0.590, and 0.512 Å). The positive and negative values mean outward and inward displacements, respectively.

16 There would be additional reasons for the absence of an end-on orientation of C_{70} in $C_{70}\subset H_4$-CPD_{Py}. The further enlargement of the dihedral angle of the two porphyrins will decrease the dihedral angles between the porphyrin planes and the meso phenyl rings of H_4-CPD_{Py}, leading to their steric repulsion. An inherently less stable end-on orientation is unlikely to occur under such an energetically severe situation.

17 M. C. Burla, R. Caliandro, M. Camalli, B. Carrozzini, G. L. Cascarano, L. De Caro, C. Giacovazzo, G. Polidori, R. Spagna, *J. Appl. Crystallogr.* **2005**, *38*, 381.

18 Crystal Structure Analysis Software, *Crystal Structure 3.8.2*, Rigaku/MSC, The Woodlands, USA, Rigaku, Japan.

19 *SHELXL-97*, Program for the refinement of crystal structures from diffraction data, University of Göttingen, Göttingen, Germany: G. M. Sheldrick, *Acta Crystallogr., Sect. A* **2008**, *64*, 112.

20 *PLATON*, A Multipurpose Crystallographic Tool: A. L. Spek, *J. Appl. Crystallogr.* **2003**, *36*, 7.